USE OF HYPER– AND MULTI–SPECTRAL IMAGING FOR DETECTION OF CHICKEN SKIN TUMORS

K. Chao, P. M. Mehl, Y. R. Chen

ABSTRACT. *Hyperspectral and multispectral imaging techniques were used to detect chicken skin tumors. Hyperspectral images of eight tumorous chickens were taken in the spectral range of 420 to 850 nm. Principal component analysis was applied to select useful wavelength bands (465, 575, 705 nm) from the tumorous chicken images. A multispectral imaging system capable of simultaneously capturing three registered images was used to image 60 tumorous and 20 normal chickens. Multispectral image analysis was performed to generate ratioed images, which were then divided into regions of interest (ROI's) classified as either tumorous or normal by a veterinarian. Image features for each ROI (coefficient of variation, skewness, and kurtosis) were extracted for use as inputs to fuzzy classifiers. The fuzzy classifiers were able to separate normal from tumorous skin with increasing accuracies as more features were used. In particular, use of all three features gave successful detection rates of 91 and 86% for normal and tumorous tissue, respectively*.

Keywords. *Food safety, Fuzzy logic, Machine vision, Poultry inspection.*

Presently, each chicken intended for sale to U.S. consumers is required by law to be inspected post–mortem by a United States Department of Agriculture/Food Safety and Inspection Service inspector (USDA/FSIS) for wholesomeness (USDA, 1984). These inspectors visually and manually inspect poultry carcasses and viscera online at processing plants. FSIS uses about 2,200 poultry inspectors to inspect roughly 8 billion chickens per year in 310 poultry slaughter plants nationwide, and this volume is growing. Each inspector is limited to a maximum of 35 birds per minute. Inspectors working at least 8 hours per day in these conditions have a tendency to develop repetitive motion injuries and attention and fatigue problems (OSHA, 1999).

Poultry inspection is a complex process. FSIS inspectors are trained to recognize infectious condition and animal diseases, dressing defects, fecal and digestive content contamination, and conditions that are related to many other consumer protection concerns. In general, diseases and defects that occur in the processing of poultry could be placed into several categories. There are diseases/defects that are localized in nature and those that are generalized or systemic; i.e. affecting the whole biological system of the bird. Systemic problems include septicemia and toxemia. Studies using visible/NIR spectroscopy (Chen et al., 2000) and reflectance imaging (Park and Chen, 1994; Chao et al., 2000) have shown good results in inspection for poultry systemic diseases. However, localized problems are difficult to detect, and require not only the use of color (spectral) information but also spatial information. Examples of localized poultry diseases/defects include skin tumors and inflammatory process. An automated system to inspect diseases/defects of poultry must be able to measure these attributes and eliminate product that is unwholesome.

Chicken skin tumors are round ulcerous lesions that are surrounded by a rim of thickened skin and dermis (Calnek et al., 1991). For high–speed inspection, machine vision is a solution, but requires advanced sensing capabilities in order to deal with the variability of a biological product. Multispectral imaging is key to these advanced techniques. Studies (Wen and Tao, 1998; Park et al., 1996; Throop and Aneshansley, 1995) have shown that the presence of defects is often more easily detected by imaging at one or more specific wavelengths where the reflectivity of good tissue is notably different from that of damaged tissue. For example, skin tumors in poultry are less reflective in the NIR than good tissue (Park et al., 1996). The measurable indication may be amplified, and therefore more easily detected, when more than one waveband is imaged and the difference or ratio of the images is measured.

The USDA's Instrumentation and Sensing Laboratory (ISL) has an ongoing program of developing real time online systems for poultry inspection. The objectives of this study were to select wavelengths for a multispectral imaging system to facilitate analysis of chicken skin tumors, to process and identify features from multispectral images, and to design classifiers for classification of normal chicken skin tissue and tumors.

Article was submitted for review in October 2000; approved for publication by the Information & Electrical Technologies Division of ASAE in November 2001.

The authors are **Kuanglin Chao,** Research Scientist, **Patrick M. Mehl,** Research Associate**,** and **Yud–Ren Chen**, **ASAE Member Engineer**, Research Leader, Instrumentation and Sensing Laboratory, USDA–ARS Beltsville Agricultural Research Center, Beltsville, Maryland. **Corresponding author**: Kuanglin Chao, USDA–ARS–ISL, Building 303, BARC–East, 10300 Baltimore Ave., Beltsville, MD 20705–2350; phone: 301–504–8450; fax: 301–504–9466; e–mail: chaok@ba.ars.usda.gov.

MATERIAL AND METHODS

EXPERIMENTAL CHICKEN CARCASSES, IMAGE MEASUREMENT SYSTEMS

A total of 80 chicken carcasses (20 normal, 60 tumorous) were collected from a poultry processing plant in Maryland

over a 2–month period in 2000. Two FSIS veterinarians identified the conditions of these chicken carcasses at the plant. The carcasses were tagged according to the condemnation categories and placed in plastic bags to minimize dehydration and color changes. The bags were then placed in coolers, filled with ice, and transported to ISL (within 2 hours) for the experiments.

Two imaging systems were used. First, a hyperspectral imaging experiment was conducted to select wavelengths for later multispectral imaging measurements. An in–house designed hyperspectral imaging system (Kim et al., 2000), which consists of a CCD camera system (SpectraVideo, PixelVision, Oreg.) equipped with an imaging spectrograph (SPECIM Inspector, Spectral Imaging, Oulu, Finland) was used for the study. The light source consists of two 21–V, 150–W halogen lamps powered with a regulated DC voltage power supply (Fiber–Lite A–240P, Dolan–Jenner Industries, Mass.). A hyperspectral image has two spatial dimensions and one wavelength dimension. The CCD camera captures the spectral dimension and one spatial dimension in a scan. The second spatial dimension is achieved by succeeding scans of a sample moved on a conveyor belt. The spatial images were 402 pixels wide perpendicular to the direction of travel of the conveyor belt and a variable number of pixels in the direction of travel, depending on the size of the chicken. This setup resulted in a spatial resolution of less than 1 mm. The wavelength dimension contained 120 points space 3.6 nm apart in the 420– to 850–nm region. Each pixel in a three–dimensional hyperspectral image has a 16–bit dynamic range.

Eight different tumorous chicken carcasses were imaged with the hyperspectral system. The samples were placed on a conveyor belt with an adjustable speed AC motor control. The image acquisition and recording was performed with a Pentium–based PC using a general–purpose imaging software package (PixelView 3.10, PixelVision, Oreg.).

After the hyperspectral imaging experiment was completed, and wavelengths selected as described below, a series of measurements was carried out with a multispectral imaging system. Chicken images (20 normal, 60 tumorous) were acquired by a multispectral imaging system consisting of a three–channel common aperture camera (TVC3, Optec, Milano, Italy), an illumination chamber, and a computer equipped with a frame grabber (XPG–1000, Dipix, Ontario, Canada). The illumination chamber was built as a box with a round–open inlet (7 cm diameter) on the top, through which the camera was mounted facing downwards. A pair of fiber optic lights (QDF5048, Dolan–Jenner Industries, Mass.) equipped with an AC–regulated 150–W quartz–halogen illuminator (PL841, Dolan–Jenner Industries, Mass.) was used for illumination. The dual lights were mounted 12 cm apart and covered with plastic light diffusers, vertical to the object. The walls of the chamber were built with optical grade black acrylic to avoid uncontrolled light reflections. Each chicken carcass was placed on a black acrylic sheet mounted to a laboratory jack for vertical position control. The image size was 728 × 572 pixels with each pixel represented a sample area of 0.1 mm^2.

The three–channel system is prism based, separating the image into three broadband images that are acquired simultaneously in the blue (B), green (G), and red (R) regions with perfect image registration. Three narrow band filters (selection described below) are placed between the prism assembly and the three CCD's, respectively, to optimize contrast between normal and tumorous areas. The images are 8 bits in each channel (gray level values of 0–255).

Hyperspectral Imaging, Wavelength Selection

Hyperspectral images were used to select wavelengths for the multispectral imaging system. Eight chicken carcasses with tumors were scanned to record spectral characteristics at each point of their surfaces. Preliminary to analysis, image processing is performed to mask the chicken, separating the chicken image from the background. Multivariate analysis utilizing the principal component analysis (PCA) was performed using the software ENVI 3.2 (Research Systems, Inc., Colo.). The PCA method is standard and may be found in the ENVI manual or an equivalent source, such as MatLab or SAS. Spatial regions of interest (ROI defined below), which contain tumors and surrounding normal skin tissue were selected. For each ROI in each chicken, the first ten principal components were extracted from the data. Each principal component was an image consisting of a weighted sum of the images at 120 wavelengths according to the formula

$$E = \sum_{i=1}^{120} w_i \lambda_i \quad (1)$$

where λ_i is the image at wavelength number i, and w_i is the weight. (E is also called an eigenvector. The different principal components or eigenvectors have different sets of weights.) The first 10 principal components (for each ROI) were visually examined, and the one providing the best contrast between tumorous and normal skin tissue was selected for that ROI. Then, for each chicken, from the set of best contrasting principal component images, the one showing the most contrast was again chosen, giving one final eigenvector (weight set) for each of the eight chickens.

The weight set corresponding to the best contrasting principal component for each chicken was then applied to the masked image for that chicken. Identification of the filters needed for multispectral imaging can be performed by analysis of the main wavelength contribution to the eigenvectors.

Multispectral Image Processing, Feature Extraction

Multispectral images are analyzed by a sequence of image processing steps to prepare for the classification. Figure 1 shows the primary steps that take place in extracting desired tumor regions from raw R, G, and B band image data (figs. 1c, b, and a, respectively). The first step is to isolate the chicken object from the rest of the image. An initial chicken mask is created by binary segmentation of the red–band chicken image with a threshold value of 40. Due to shading and shape of the chicken surface some internal holes and noise regions in the background still remain in the initial mask. The majority of such unwanted pixels can be removed and/or filled with a series of morphological operations (Dougherty, 1992). Small regions of background noise pixels are first removed through a 7 × 7 opening operation. A 10 × 10 closing operation, followed by a 3 × 3 erosion operation is performed to fill the internal holes and smooth the edges of the chicken mask. An example of the final chicken mask can be seen in Figure 1d.

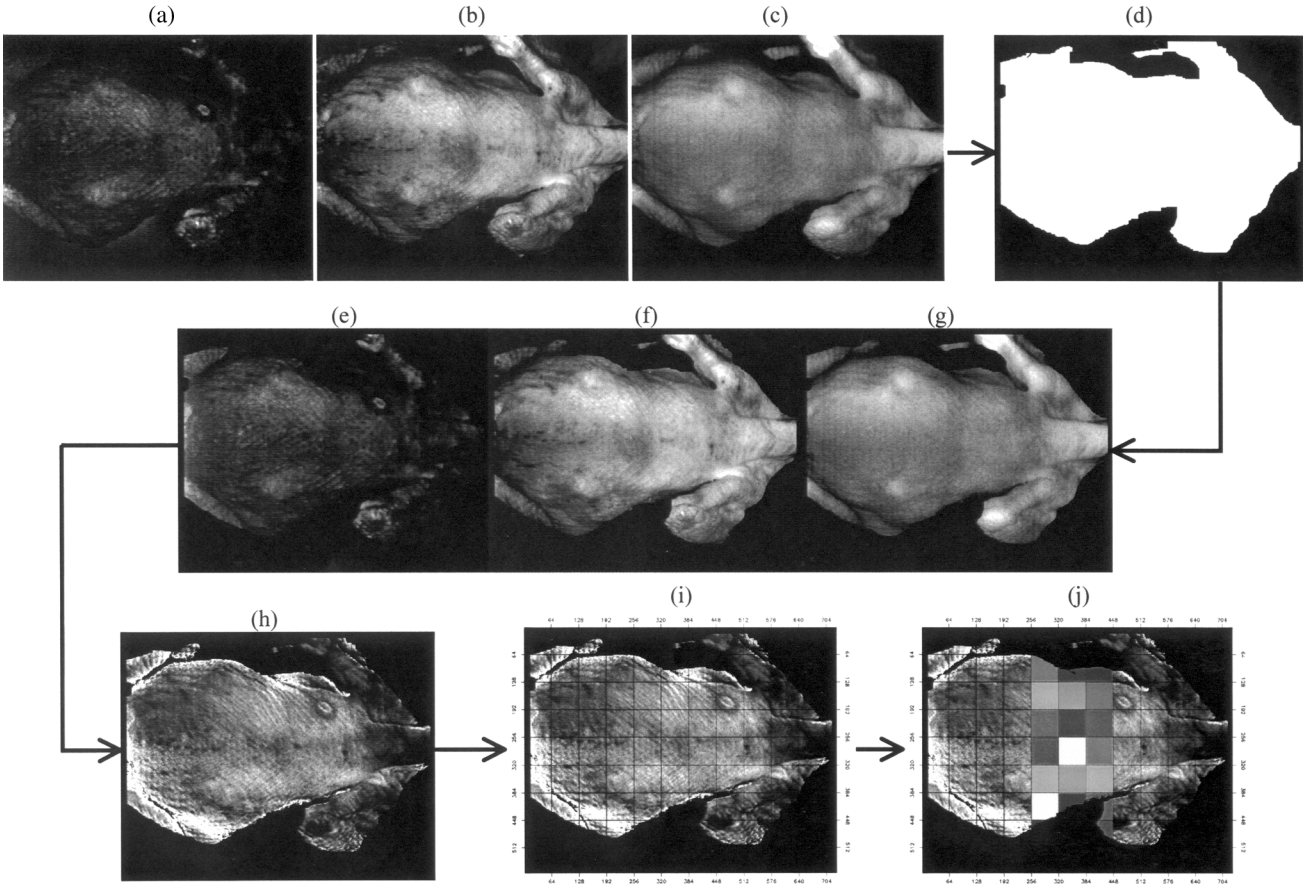
(a)
(b)
(c)
(d)
(e)
(f)
(g)
(h)
(i)
(j)

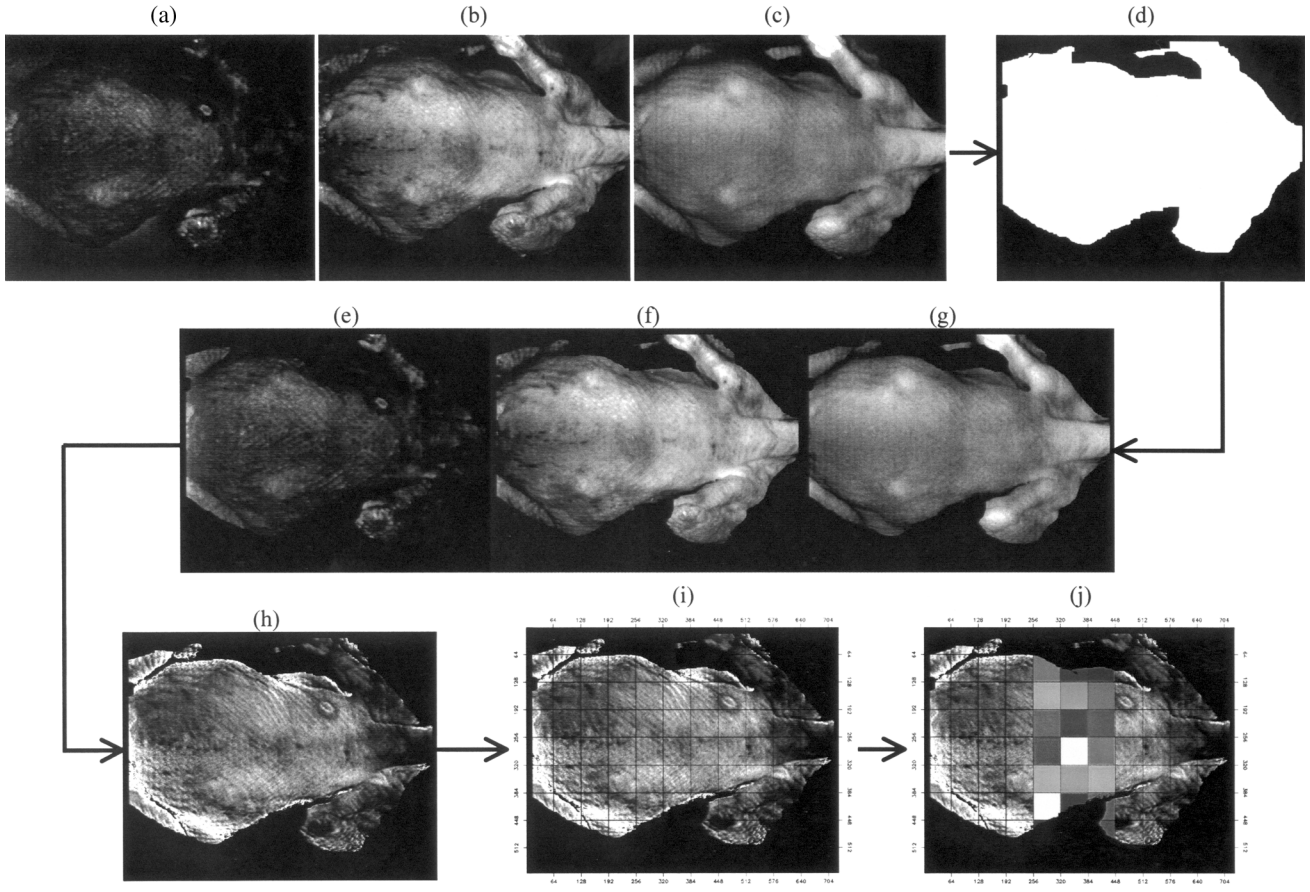

Figure 1. Multispectral image processing. (a, b, c) Raw images from B,G,R channels, (465–, 575–, 705–nm bands). (d) Mask developed from red channel. (e, f, g) Images a, b, c after application of mask. (h) Band combination (B/2+G/2)/R. (i) Grid generation. (j) ROI generation.

After the chicken mask is created all analyses and operations are limited to only those pixels within the mask. Figures 1g, f, and e illustrate masked chicken images in the filtered red (R), green (G), and blue (B) channels, respectively. It is clearly shown that chicken images are presented differently in R, G, and B channels. Chicken skin tumor is clearly presented in the B–channel. Lesions including skin tumor, cuts, and blood clots are exposed in the G–channel. However, in the R–channel chicken skin is smooth without showing lesions. Therefore, the three–channel images can be combined to generate one image for feature extraction of chicken skin tumor. A combination was chosen to average the B– and G– channels that showed defects of interest. The combination then included a division by the R–channel, in order to reduce unimportant image variation. The ratioed image of [(G/2) + (B/2)] / [R] is shown in figure 1h.

A square grid with a mesh size of 64 × 64 (4096 pixels) was placed over each image. The intersection of a square with the masked chicken image was called a ROI (region of interest). (ROI's containing the edge of the masked chicken image contains less than 4096 pixels.) ROI's were classified into two categories, normal and tumorous, based on the veterinarian's judgment. ROI's classified as normal came from the 20 normal chickens and non–tumorous areas of the 60 tumorous chickens, for a total of 778 "normal" ROI's. "Tumorous" ROI's totaled 103 from tumorous areas of the tumorous chickens. A training set of ROI's (100 normal and 52 tumorous) was randomly extracted from the database. This training set includes roughly half of the tumorous ROI's. Only 100 of the normal ROI's were used in order to make the numbers of normal and tumorous more equal, resulting a more even distribution of the Type I and Type II errors. The seven classification configurations (defined below) trained on this subset of 152 samples were then applied to the testing set consisting of the remaining 729 samples (678 normal and 51 tumorous).

The classification was based on features extracted from variations in the ratioed intensities within each ROI. These variations are exploited as image features using the first four statistical moments (mean, standard deviation, skewness, and kurtosis, the first two combined into coefficient of variation).

For each defined ROI, statistical moments are calculated on the basis of reflectance intensity. The statistical computation provides mean, variance, standard deviation, skewness, and kurtosis of a sample population contained in an n–element vector X (reflectance intensities). With $x = (x_o, x_{1,} x_{2,} \ldots, x_{n-1})$, the various moments can be calculated as follows:

$$Mean = \bar{x} = \frac{1}{N} \sum_{j=0}^{N-1} x_j \quad (3)$$

$$Variance = \frac{1}{N}\sum_{j=0}^{N-1}(x_j - \bar{x})^2 \quad (4)$$

$$Standard\ Deviation = \sqrt{Variance} \quad (5)$$

$$Skewness = \frac{1}{N}\sum_{j=0}^{N-1}\left(\frac{x_j - \bar{x}}{\sqrt{Variance}}\right)^3 \quad (6)$$

$$Kurtosis = \frac{1}{N}\sum_{j=0}^{N-1}\left(\frac{x_j - \bar{x}}{\sqrt{Variance}}\right)^4 - 3 \quad (7)$$

The image features of coefficient of variation (CV, defined as (standard deviation / mean) × 100), skewness, and kurtosis are evaluated in this study. Software programs were developed using the IDL programming language (Research Systems, Colo.) for processing the multi–spectral images.

Multispectral Image Classification

A general–purpose fuzzy inference system (Chao et al., 1998) was applied to classify chicken skin tissue into normal and tumor. The fuzzy inference process was implemented with three operations: (1) fuzzify numerical inputs (e.g. CV, skewness, kurtosis) using input membership functions; (2) apply fuzzy operators to the antecedents of the rule base; (3) perform implication, i.e. evaluate the consequent portion of the rules. Step one operation is to translate the measured numerical values of the image features into linguistic values with corresponding membership grades. A set of membership functions was constructed based on partition of subspaces from correspondence graphs between image features. The membership functions design allows the boundary between two neighboring classes to form an overlapping area, so that a feature has partial membership grades in each class. A rule base maps linguistic inputs to outputs. Each fuzzy characterization rule in the rule base can be viewed as a conditional statement in the form of:

If (image feature measurements) *Then* (characterization) (8)

The condition part of a rule consists of image features (e.g. CV, skewness, kurtosis) of the chicken skin tissue. The characterization part of a rule is a linguistic class name, such as normal and tumor. Based on the result of pattern matching between rule antecedents and input features, a number of fuzzy rules are triggered in parallel with various values of firing strength. The fuzzy process quantifies these actions. The fuzzy inference engine, employing a combination of max and min operations, can then be applied to determine the level of certainty for pattern classification.

$$\mu_{CLASS}(C_k) = \max \min(\mu_{F1i}(x_{P1}), \mu_{F2j}(x_{P2}), \ldots, \mu_{Fnk}(x_{Pn})) \quad (9)$$

where $\mu_{CLASS}(C_k)$ are the output membership grades for normal (C_1) and tumor (C_2); $\mu_{F1i}(x_{P1})$, $\mu_{F2j}(x_{P2})$, . . ., $\mu_{Fnk}(x_{Pn})$ are the membership grades for the input features. The minimum operator is used to limit the certainty of the overall condition to that of the least certain observation. If the same characterization is prescribed by more than one selected rule, its certainty is set to the maximum of the individual rules. Then the collection of these possible characterization forms the following fuzzy set:

$$CLASS = \{\mu_{CLASS}(C_1)/C_1, \mu_{CLASS}(C_2)/C_2\} \quad (10)$$

The Fuzzy Logic Toolbox (Mathworks Inc., Natick, Mass.) was used to design the fuzzy classifiers.

Results and Discussion

Wavelength Selection

Hyperspectral image data was analyzed for the first 10 PCA bands to select bands presenting the best contrast and differences between tumors and normal skin tissue of the chicken. The PCA bands varied depending on the amount of statistical information presented by the chickens. The selection of the more efficient PCA bands provided the determination of eigenvectors and eigenvalues corresponding to the PCA bands and the associated statistical analysis.

Figure 2 shows the weighed wavelengths distribution corresponding to the eigenvector defined on chicken skin tumors that provided the best contrast between tumors and normal chicken skin. Two significant bands were observed: 475±50 nm and 575±50 nm with low level of contribution from the near infrared region. These bands correspond to metmyoglobin and oxymyoglobin bands (Liu et al., 2000). Direct near infrared region provided no information for the presence of chicken skin tumor. The near infrared region was not sensitive for the surface defects on the chicken (Park et al., 1996). It can therefore be utilized as an invariant image for masking and normalization of chicken carcass images. A filter at 705 nm was chosen to achieve this. Selection of the wavelengths with the filters for the multispectral imaging system using an adaptable three–band CCD camera included the following: 465±10 nm, 575±10 nm, and 705±10 nm. (The ±10 nm designates the full–width–at–half–maximum band–pass.)

Multispectral Image Features

Figure 3 shows the correspondence between skewness and coefficient of variation (CV) for normal skin tissues and tumors. Data indicates that normal tissues have lower CV than tumors. There was no normal skin tissue observed for

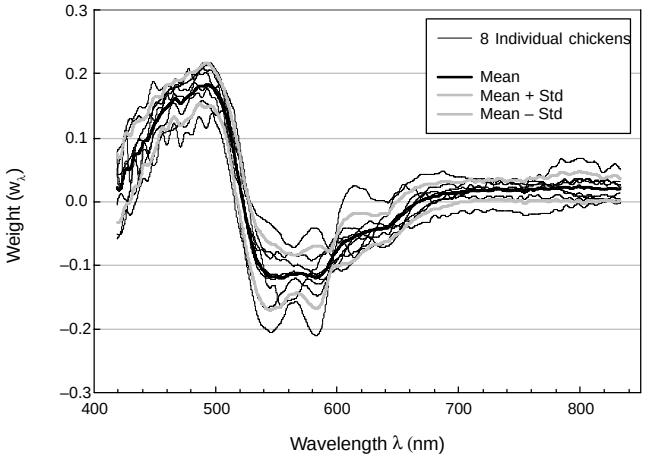

Figure 2. Final eigenvectors for each of eight chickens, from hyperspectral image analysis.

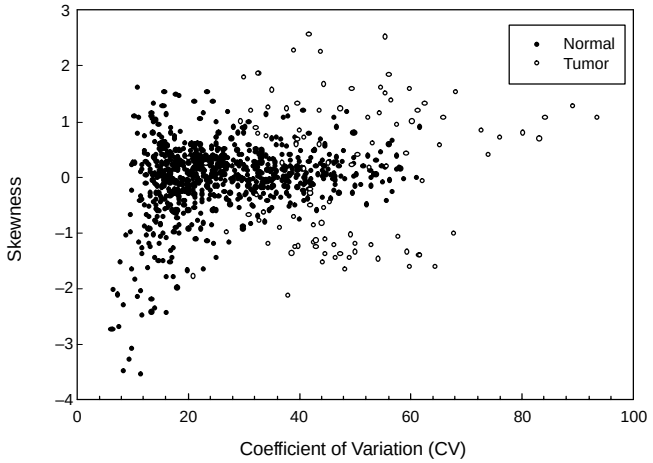

Figure 3. Relationship between coefficient of variation and skewness for normal and tumorous classes.

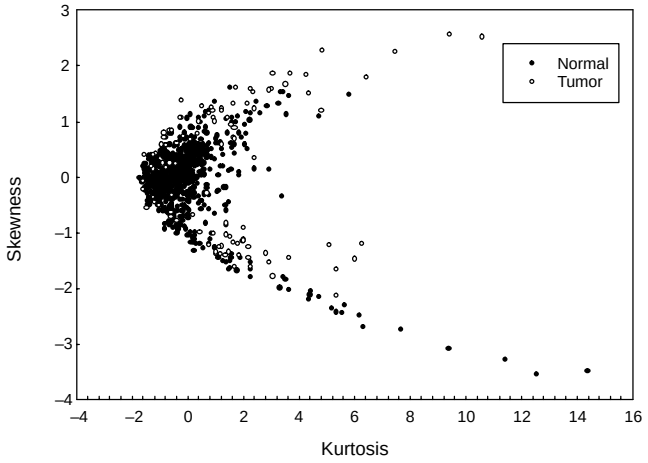

Figure 5. Relationship between skewness and kurtosis for normal and tumorous classes.

CV above 64. This observation arises from the high reflectance intensity variation existing between exposed muscle from the tumor center, the surrounding connective tissue, and discolored (yellowish) skin. Similarly there was no tumor observed for CV below 20. For this region, highly negative skewness values are present due to the intensity saturation for bright spots. The maximum skewness values were higher for tumors than for normal tissue for CV between 20 and 64 because some discolored skin tissues exhibited lower reflectance intensity in the blue–channel region and displaced the peak of intensity distribution to the lower left hand compared to normal skin tissue.

Figure 4 shows kurtosis versus CV for tumors and normal tissues. In general, kurtosis was centered around zero for normal chicken. As expected, kurtosis presented positive high value for normal chicken skin tissue in bright spots. Similar to skewness in figure 3, tumor presented high kurtosis value for CV above 20. Figure 5 shows skewness and kurtosis for normal skin tissue and tumors are distributed along a parabolic curve. Normal skin tissues have lower skewness value than tumors (as seen in fig. 3). However, the data shown in figure 5 reveals the difficulty of separating normal skin tissue and tumor using only skewness and kurtosis. This pattern may come from slight amounts of tumors in ROI's assigned to the normal category.

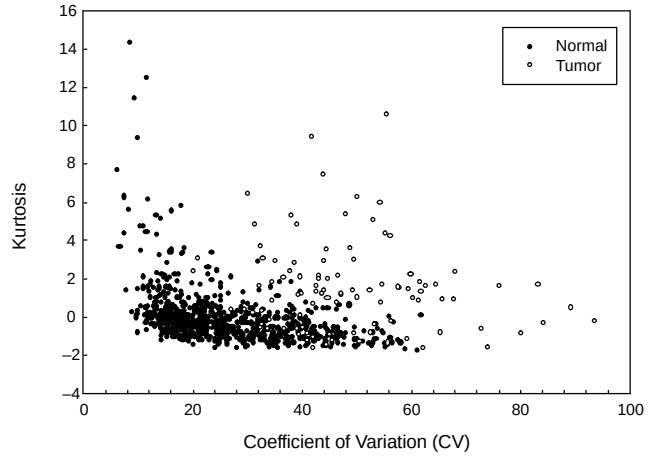

Figure 4. Relationship between coefficient of variation and kurtosis for normal and tumorous classes.

CLASSIFICATION

The fuzzy classifiers are based on the observations noted above. Figure 6 shows the membership functions for chicken skin tumor classification. The fuzzy sets for the CV were derived from data interpretation, i.e. no skin tumor observed for CV below 20 and no normal skin tissue observed for CV above 64. A fuzzy set with normal distribution (labeled medium) was designed to cover CV between 20 to 70. These fuzzy sets were overlapped between two neighboring classes, proving partial membership in each class. A similar approach was applied to derive fuzzy sets for the skewness. For the feature kurtosis, two fuzzy sets were implemented. Based on these fuzzy sets, the fuzzy classifier can be described by a set of fuzzy rules. The following six rules (using CV and skewness) were generated for classification of chicken skin tumors:

R1: if (CV is low) and (skewness is medium) then (normal).
R2: if (CV is low) and (skewness is high) then (normal).
R3: if (CV is medium) and (skewness is low) then (tumor).
R4: if (CV is medium) and (skewness is medium) then (normal).
R5: if (CV is medium) and (skewness is high) then (tumor).
R6: if (CV is high) then (tumor).

For testing the fuzzy classifier, features of CV, skewness, and kurtosis were first applied individually. Then pairs of features were applied (three configurations), followed by one configuration using all three features.

Table 1 compares the accuracy of fuzzy classifiers when features of individual moments and combined moments were used for classification of chicken skin tumor. Training results were somewhat better than testing results, as is usually the case. Both training and testing results showed improvement when more features were used. Only the testing results will be discussed because they represent a more realistic estimate of a calibration's future performance. The classification accuracy for skin tumor varied from 31 to 64% when individual features were used as input to the fuzzy classifier. This variation in accuracy indicated that individual features couldn't be effectively used for chicken skin tumor classification. The tumor classification accuracy was improved to 86% when combined features of CV, skewness,

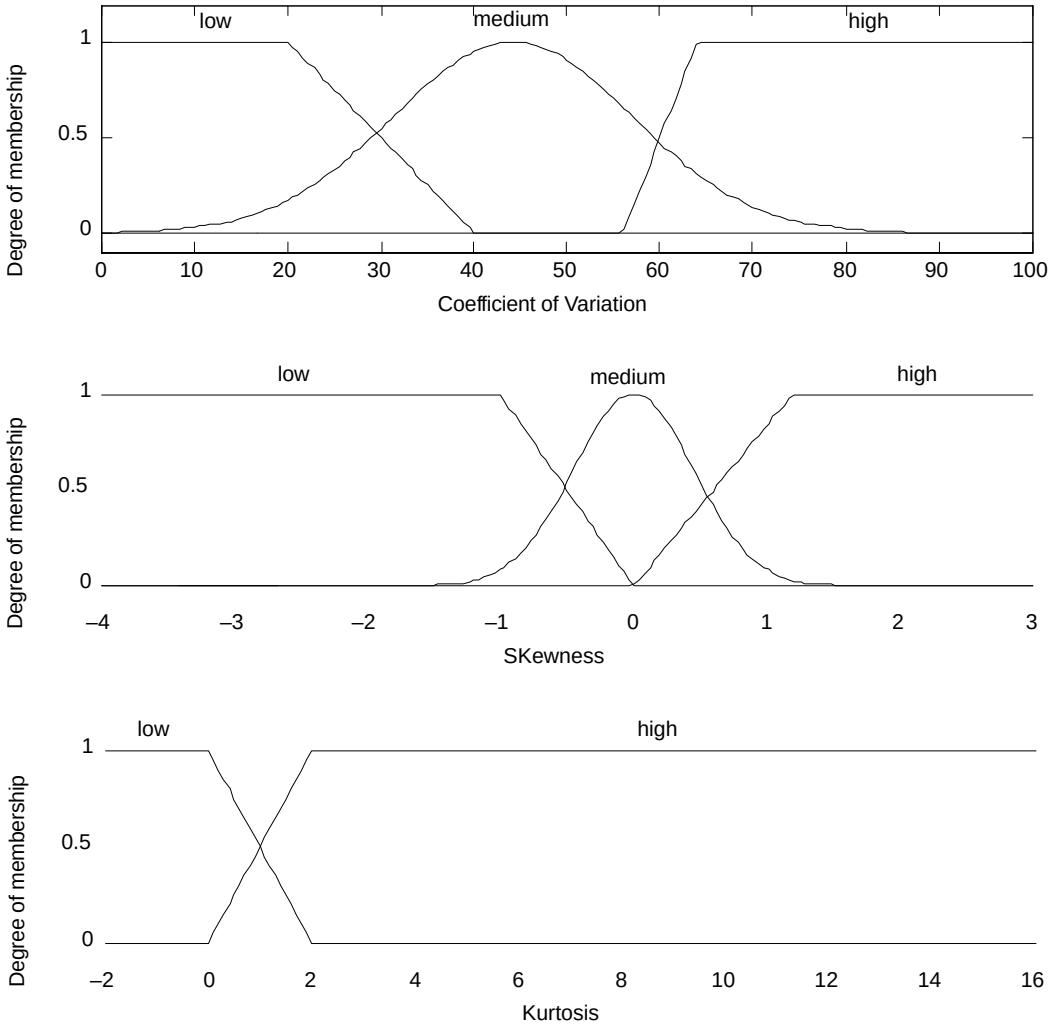

Figure 6. Membership functions for chicken skin tumor classification.

and kurtosis were used. The corresponding accuracy for normal ROI's, using the combined features, was 91%. Comparing the results from different features, the combination of CV, skewness, and kurtosis yielded the highest rate of correct classification.

Table 1. Correct classification rate of fuzzy classifier using different features.

	Normal	Skin Tumor	
Coefficient of variation	81% (81/100)	69% (36/52)	Training
	80% (542/678)	64% (33/51)	Testing
Skewness	87% (87/100)	42% (22/52)	Training
	83% (566/678)	31% (16/51)	Testing
Kurtosis	92% (92/100)	69% (36/52)	Training
	84% (568/678)	63% (32/51)	Testing
Coefficient of variation, Skewness	82% (82/100)	81% (42/52)	Training
	78% (529/678)	78% (40/51)	Testing
Coefficient of variation, Kurtosis	86% (86/100)	75% (39/52)	Training
	84% (570/678)	63% (32/51)	Testing
Skewness, Kurtosis	90% (90/100)	69% (36/52)	Training
	84% (568/678)	65% (33/51)	Testing
Coefficient of variation, Skewness, Kurtosis	92% (92/100)	88% (46/52)	Training
	91% (620/678)	86% (44/51)	Testing

CONCLUSIONS

Chicken carcass images were examined by hyper– and multi–spectral based image analysis. Principal component analysis of ROI's of hyperspectral images of normal and tumor areas provided the basis for selection of three narrow–band wavelength regions for use in a common aperture multi–spectral imaging system. Feature extraction from the variability of ratioed multi–spectral images, including mean, standard deviation, skewness, and kurtosis, provided the basis for fuzzy logic classifiers, which were able to separate normal from tumorous skin areas with increasing accuracies as more features were used. In particular, use of all three features gave successful detection rates of 91 and 86% for normal and tumorous tissue, respectively. These

levels of classification accuracy would be useful in an online inspection facility.

REFERENCES

Calnek, B. W., H. J. Barnes, C. W. Beard, W. M. Reid, and H. W. Yoder. 1991. *Diseases of Poultry*, 386–484. Ames, Iowa: Iowa State University Press.

Chao, K., B. Park, Y. R. Chen, W. R. Hruschka, and F. W. Wheaton. 2000. Design of a dual–camera system for poultry carcasses inspection. *Applied Engineering in Agriculture* 16(5): 581–587.

Chao, K., R. S. Gates, and R. G. Anderson. 1998. Knowledge–based control systems for single stem rose production – Part I: systems analysis and design. *Transactions of the ASAE* 41(4): 1153–1161.

Chen, Y. R., W. R. Hruschka, and H. Early. 2000. A chicken carcass inspection system using visible/near–infrared reflectance: in plant trials. *J. of Food Process Engineering* 23(2): 89–99.

Dougherty, E. R. 1992. *An Introduction to Morphological Image Processing*, 17–26. Bellingham, Wash.: SPIE Optical Engineering Press.

OSHA. 1999. Chicken disassembly – ergonomic considerations. http://www.osha–slc.gov/SLTC/poultryprocessing. U.S. Department of Labor, Washington, D.C.

Kim, M. S., K. Chao, Y. R. Chen, D. Chan, and P. M. Mehl. 2000. Hyperspectral imaging system for food safety: detection of fecal contamination of apples. *Proc. SPIE*, 4206: 174–184. Bellingham, Wash.: SPIE Optical Engineering Press.

Liu, Y., Y. R. Chen, and Y. Ozaki. 2000. Characterization of visible spectral intensity variations of wholesome and unwholesome chicken meats with two–dimension spectroscopy. *Applied Spectroscopy* 54(4): 587–594.

Park, B., and Y. R. Chen. 1994. Intensified multi–spectral imaging system for poultry carcass inspection. *Transactions of the ASAE* 37(6): 1983–1988.

Park, B, Y. R. Chen, M. Nguyen, and H. Hwang. 1996. Characterizing multispectral imagings of tumors, bruised, skin–torn, and wholesome poultry carcasses. *Transactions of the ASAE* 39(5): 1993–1941.

Throop, J. A., and D. J. Aneshansley. 1995. Detection of internal browning in apples by light transmittance. *Proc. SPIE* 2345: 152–165. Bellingham, Wash.: SPIE Optical Engineering Press.

USDA. 1984. A review of the slaughter regulations under the Poultry Products Inspection Act. Regulations Office, Policy and Program Planning, FSIS, USDA, Washington, D.C.

Wen, Z., and Y. Tao. 1998. Fuzzy–based determination of model and parameters of dual–wavelength vision system for on–line apple sorting. *Optical Engineering* 37(1): 293–299.